

# CRAMÉR-RAO BOUNDS FOR THE LOCALIZATION OF ANISOTROPIC SOURCES

*E. Monier and G. Chardon*

Laboratoire des Signaux et Systèmes (L2S),  
CentraleSupélec, CNRS, Univ Paris Sud, Université Paris-Saclay,  
3 rue Joliot-Curie, 91192 Gif-sur-Yvette, France

## ABSTRACT

In the most general case, source localization has to take into account the radiation pattern of the sources of interest. This is particularly important when the sensors surround the sources, and the sources are anisotropic, as is the case in several applications (EEG, speech, musical instruments, etc.). Cramér-Rao bounds for the joint estimation of the position of a source and its radiation pattern are computed for simple cases of sensor array geometries and source models, showing that a good match between the source and the model improves the Cramér-Rao bounds. It is also shown that, in general, using a model more complex than the source makes the Fisher information matrix singular. These results are supported by numerical simulations and physical interpretations.

**Index Terms**— Source localization, Cramér-Rao bounds, multipoles, acoustic imaging

## 1. INTRODUCTION

Most of source localization methods are concerned with far-field sources. In this case, only the direction of arrival of the source is to be estimated. The radiation pattern of the source is neglected, as it can be considered constant over the angle spanned by the sensor array relative to the source. However, true isotropic sources (or monopolar sources) are the exception. Most sources have a non-isotropic radiation pattern.

Examples include:

- Electroencephalograms (EEG), where sources are dipoles
- turbulence noise, radiating like a quadrupole [1]
- electroacoustic sources, such as unbaffled (radiating as dipoles) or cardioid speakers
- sound radiated by an exploding bubble (dipole)
- human voice[2]
- scattering of a electromagnetic or acoustic plane wave by an object.

When the sensor array is in the near-field of the sources, or when the sensors surround the sources, it is no longer possible to neglect the anisotropy of the radiation pattern.

In this case, the position of the sources *and* the radiation pattern have to be jointly estimated. Several methods can be used for this estimation problem:

- generalizations of the MUSIC (MUltiple SIgnal Classification) algorithm [3, 4]

---

EM is now in IRIT (INPT, UPS, UT2J, UT1, CNRS), 118 route de Narbonne F-31062 Toulouse, CEDEX 9

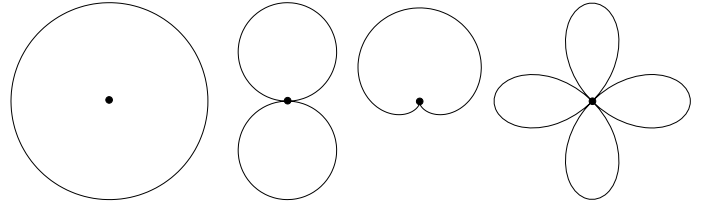


**Fig. 1.** Radiation pattern of monopolar, dipolar, cardioid and quadrupolar sources.

- or group-sparsity models and corresponding identification methods (mixed-norms, block matching pursuits, etc.) [5].

In this paper, we compute the Cramér-Rao bounds for the joint estimation of the position and the radiation pattern of a source. Exact results are obtained in a simplified setting. It is shown that not only the variance of the position estimator increases with the complexity of the source, but also that a mismatch between the radiation model and the actual source (i.e. when the model is more complex than the source) makes the Fisher information matrix of the estimation problem singular. This last result is proved in the general case.

### 1.1. Previous works

The radiation pattern is explicitly taken in account in some EEG localization methods. In particular, Cramér-Rao bounds for the localization of current dipoles in the skull are given in [6]. Results are however limited to pure dipoles.

Several papers have recently appeared on acoustic source localization in reverberant rooms [7, 8, 9, 10]. While these papers deal with the reverberation (known or unknown), no method is given to deal with anisotropic radiation patterns. Such radiation patterns are expected for a large number of type of sources (human voice, musical instruments, aerodynamic noise, etc.), and the geometry of the problem (sensors close to the sources, reverberation) makes the usual assumption of monopolar source irrelevant. The method introduced in [8] is also applied to EEG. The authors suggest to approximate a dipole as the sum of two close out-of-phase monopoles. However, as the space is discretized on a regular grid, only dipole aligned with the axes can be approximated as a sum of two monopoles, making the interpretation of the results difficult.

MUSIC-type algorithms are introduced in [3, 4]. Some conditions on the number of measurements and snapshots are given in [4], however, the variance of the estimators is not considered.

## 1.2. Structure of the paper

The physical source model is introduced in section 2. Values of the Cramér-Rao bounds for some special cases of sources and measurement setups, as well as a general result on the invertibility of the Fisher matrix of the estimation problem are given in section 3. Simulation results are discussed in section 4, and concluding remarks are given in section 5.

## 2. SOURCE MODEL

The field radiated by a source at the origin can be decomposed as a sum of multipoles [11]. The multipoles are the solutions of the Helmholtz equation with a Dirac, or a high order derivative of a Dirac, as right-hand side. The multipole of order  $(l, m)$  (with  $|m| \leq l$ ) is given in spherical coordinates by:

$$S_{lm}(r, \theta, \phi) = Y_{lm}(\theta, \phi) h_l(kr)$$

where  $Y_{lm}$  is the spherical harmonic of order  $(l, m)$ ,  $h_l$  is the spherical Hankel function of order  $l$  (Definitions and properties of the Bessel and Hankel functions are found in [12]) and  $k$  the wavenumber. In particular, the multipole of order  $(0, 0)$  is the well known Green function  $S_{00}(r, \theta, \phi) = \frac{e^{ikr}}{r}$ . In the 2D case, the multipole of order  $l$  has the simple expression in polar coordinates

$$S_l(r, \theta) = e^{il\theta} H_l(kr)$$

where  $H_l$  is the cylindrical Hankel function of order  $l$ .

A source is described by the coefficients  $a_{lm}$  (or  $a_l$ ) of its expansion in the family of multipoles. The field  $u$  radiated by the source (in 3D or 2D) is decomposed as:

$$u(r, \theta, \phi) = \sum_{l=0}^{\infty} \sum_{m=-l}^l a_{lm} Y_{lm}(\theta, \phi) h_l(kr)$$

$$u(r, \theta) = \sum_{l=-\infty}^{\infty} a_l e^{il\theta} H_l(kr).$$

From now on, for the sake of simplicity, only 2D sources will be considered. As the results described in this paper are based on properties that are shared by 2D and 3D multipoles (expression of the derivative of a multipole of order  $n$  as a sum of multipoles of order  $n-1$  and  $n+1$ , as well as the Graf theorem [13]) and not on their exact expressions, the results can be readily applied to the 3D setting.

Here are some examples of sources (if unspecified,  $a_l$  is assumed to be zero)[11]:

- $a_0 \neq 0$ : monopolar, omnidirectional source.
- $|a_1| = |a_{-1}| \neq 0$ : figure-of-eight radiation pattern. Its orientation depends on the relative phase between  $a_1$  and  $a_{-1}$ .
- $|a_1| = |a_{-1}| = |a_0|/2 \neq 0$ , cardioid radiation pattern.
- $|a_2| = |a_{-2}| \neq 0$ : quadrupolar pattern.

More complex models include musical instruments, Yagi antennas, scattering by an object, etc, where higher order multipoles are involved. In the following section, a subset of multipoles will be used to describe a source and estimate its position, and the amplitudes of the chosen multipoles.

## 3. CRAMER-RAO BOUNDS

Given a quantity to be estimated, the Cramér-Rao bounds give a lower bound for the variance of any unbiased estimator of this quantity. They are obtained by inverting the Fisher information matrix (FIM). Assuming that the measurements are corrupted by a centered white Gaussian noise of variance  $\sigma^2$ , the terms of the FIM are given by

$$F_{ij} = \frac{1}{\sigma^2} \text{Re} \frac{\partial \mathbf{m}}{\partial \theta_i}^H \frac{\partial \mathbf{m}}{\partial \theta_j}$$

where  $\mathbf{m}$  is the vector of the values of the field radiated by a source to the sensors in function of the parameters  $\theta_i$  (position and amplitudes), i.e.  $u(r, \theta)$  sampled at the sensors positions.  $\cdot^K$  denotes conjugate transpose.

### 3.1. Simplifying assumptions

To avoid overcomplicated computations and allow a simple interpretation of the results, simplifying assumptions will be made for the computation of the Cramér-Rao bounds. We will consider a uniformly sampled circular array of  $N$  sensors, with the sources placed at the center of the array. For coefficients  $a_l$  nonzero up to  $|l| \leq L$  and a sufficient number of sensors  $N \leq 2L + 3$ , multipoles are orthogonal, yielding simple expressions for the coefficients of the Fisher information matrix.

In the following, the squared magnitude of a complex number  $a = a_r + ia_i$  will be denoted with an upper case letter  $A = a_r^2 + a_i^2$  (similar notations will be used for  $B$  and  $C$ ).

### 3.2. Monopolar source

In the monopolar case, the source is describe by the real part  $a_r$  and imaginary part  $a_i$  of its amplitude, and its position  $(x, y)$ . the FIM writes

$$F = \frac{N}{\sigma^2} \begin{pmatrix} h_0 & & & \\ & h_0 & & \\ & & k^2 A h_1/2 & \\ & & & k^2 A h_1/2 \end{pmatrix} \begin{bmatrix} a_r \\ a_i \\ x \\ y \end{bmatrix}.$$

The Cramér-Rao bound for the estimation of the position of the source is thus

$$CRB_x = CRB_y = \frac{2\sigma^2}{ANk^2} \frac{1}{h_1}.$$

### 3.3. Pure dipole

A pure dipole is described by six parameters: the coefficients of the multipoles of order  $-1$  and  $1$  ( $a_r, a_i, b_r, b_i$ ), and its position:

$$u(r, \theta) = (a_r + ia_i)e^{-i\theta} H_{-1}(kr) + (b_r + ib_i)e^{i\theta} H_1(kr).$$

The FIM for the parameters  $a_r, a_i, b_r, b_i, x, y$  is a block diagonal matrix:

$$F = \frac{N}{\sigma^2} \begin{pmatrix} h_1 I_4 & \\ & k^2 F_{xy}/4 \end{pmatrix}$$

where

$$F_{xy} = (A + B)(h_0 + h_2)I_2 + 2h_0 \begin{pmatrix} -a_r b_r - a_i b_i & -a_r b_i + a_r b_i \\ -a_r b_i + a_r b_i & +a_r b_r + a_i b_i \end{pmatrix}$$

and  $I_n$  is the  $n \times n$  identity matrix. In the particular case where  $a = b$  is real (i.e. the dipole is oriented along the  $y$  axis and the FIM is diagonal), the Cramér-Rao bounds for the position writes

$$CRB_x = \frac{2\sigma^2}{ANk^2} \frac{1}{h_2}$$

$$CRB_y = \frac{2\sigma^2}{ANk^2} \frac{1}{2h_0 + h_2}.$$

For large  $r$ , where  $|H_0(kr)| \approx |H_1(kr)|$ , we get

$$CRB_x \approx 3CRB_y.$$

A physical interpretation can be given for this difference in variance in the two directions. If the dipole is moved along the  $x$  direction, no change is measured by the sensors on the  $x$  axis, while only a small amplitude change is measured by sensors on the  $y$  axis. However, if is moved along the  $y$  axis, the power received by the sensors on the  $x$  axis increases, while the displacement on the  $y$  axis implies a phase change on the sensors near the  $y$  axis, where the power is maximal and thus less sensible to noise. As a displacement along the  $y$  axis modifies the received field on the sensors more than a displacement along the  $x$  axis, estimation of the position along  $y$  is potentially better.

### 3.4. Higher order sources

Higher orders (quadrupoles, octopoles, and more) are described by:

$$u(r, \theta) = (a_r + ia_i)e^{-il\theta}H_{-l}(kr) + (b_r + ib_i)e^{il\theta}H_l(kr)$$

with  $l > 1$ . They yield a diagonal Fisher information matrix, and a Cramér-Rao bound of value  $\sigma^2 k^2 / (N(A + B)h_{l+1})$  for  $x$  and  $y$  positions. In contrast to the dipole case, higher order sources have equal Cramér-Rao bounds for the two directions.

### 3.5. Mixture of monopole and dipole

Some sources (e.g. human voice, cardioid loudspeakers, etc.) are described by a mixture of a monopole and a figure of eight dipole:

$$u = (a_r + ia_i)e^{-i\theta}H_{-1}(kr) + (b_r + ib_i)H_0(kr) + (c_r + ic_i)e^{i\theta}H_1(kr).$$

In this case, depending on the amplitudes of the multipoles describing the source, off-diagonal coefficients appear in the FIM, coupling the position and the amplitudes. These couplings have important consequences on the FIM.

If the source is actually a pure monopole (i.e. if the amplitudes of the dipoles are both zero), the FIM is singular. A singular FIM implies that no unbiased estimator with finite variance exists [14].

If the source is a pure figure-of-eight dipole (i.e.  $A = C$  and  $B = 0$ ), this coupling implies that the Cramér-Rao bounds in  $x$  and  $y$  direction are equal:

$$CRB_x = CRB_y = \frac{2\sigma^2}{ANk^2} \frac{1}{h_2}$$

yielding a larger position estimation error than estimation using a dipole only model.

Similar results are obtained for a mixture of monopole, dipoles and quadrupoles, i.e. that compared to a pure quadrupolar model, variance is increased for a pure quadrupole source, and that the FIM is singular if the source does not radiate a quadrupole.

### 3.6. A general result

The main result of the study of the Cramér-Rao for the particular cases exposed above is the fact that the FIM is singular in the cases where the model is more complex than the source, i.e. that multipoles of orders  $L$  are included in the model while the source does not radiates energy for these multipoles.

This property of the FIM is not limited to these simple cases. Given a combination of multipoles

$$u = \sum_{l=-L}^L a_l e^{il\theta} H_l(kr),$$

we have

$$\frac{\partial u}{\partial x} = \frac{k^2}{2} \sum_{l=-L}^L a_l (e^{i(l-1)\theta} H_{l-1}(kr) - e^{i(l+1)\theta} H_{l+1}(kr)).$$

and

$$\frac{\partial u}{\partial a_l} = e^{il\theta} H_l(kr).$$

In the case where  $a_{-L} = a_L = 0$ , the spatial derivative is a linear combination of the amplitude derivatives, implying that the corresponding column of the FIM is a combination of the columns associated to the amplitudes. In this case, the FIM is singular. A identical result is obtained for the position  $y$ .

## 4. SIMULATION RESULTS

In this section, simulation results corresponding to the particular cases exposed above are given. Sources are located by the maximum likelihood estimator. The position with the higher likelihood is such that the angle between the measurements and the space spanned the elementary sources centered at that point is minimum (in the case of a simple, monopolar source, it is similar to taking the maximum of a standard beamformer output).

We consider a circular array of 10 sensors, uniformly located on a circle of radius 10m. Two sources, a monopole and a dipole, are considered, at frequency 1kHz.

Results are given for the estimation of the position of a monopolar and a dipolar source, for increasingly complex models. In the different models, the amplitudes of the elementary sources are one, and the variance of the noise  $\sigma^2$  is constant. This yields different values of the SNR for the different models.

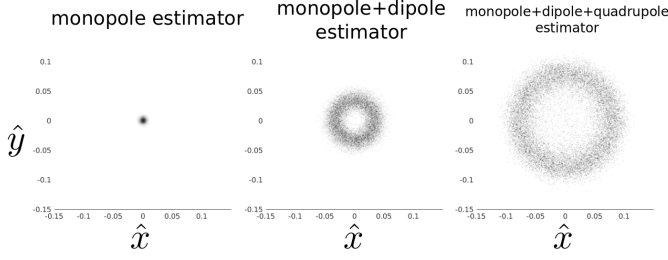
These simulations highlight the effect of an overestimation of the model order:

- the variance of the estimation of the position is increased,
- the probability density of the estimation lies around a circle of increasing radius with increasing order, and is low at the actual position of the source,
- the estimation of some parameters is biased, e.g. the amplitude of a pure monopole using a monopole+dipole model.

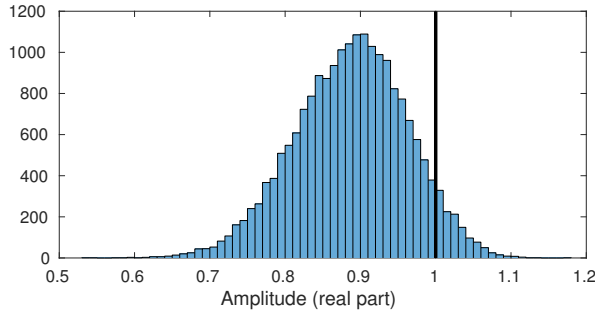
### 4.1. Monopole

Figure 2 show the scatter plot of the estimated  $x$  position of a source located at the center of the sensor array, for 3 different source models:

- monopolar source,
- mixture of monopole and dipole,



**Fig. 2.** Estimations of the position of a monopole using models of increasing complexity.



**Fig. 3.** Histogram of the estimation of the amplitude for a monopole, using a monopole + dipole model. True amplitude indicated by the vertical line.

- mixture of monopole, dipole and quadrupole.

with  $\text{SNR} = 17\text{dB}$ . The variance of the estimated  $x$  position is clearly increasing with the complexity of the model. It is also shown that for complex models, the estimation position lies on a circle of diameter increasing with the complexity.

Figure 3 shows an histogram of the estimation of the real part of the amplitude of the monopole for the monopole + dipole model. In coherence with the fact that the FIM is singular, a large estimation bias is visible.

#### 4.2. Dipole

Similarly, the position of a dipole located at the center is estimated with three different models: pure dipole model, and the same mixture models used above, with  $\text{SNR} = 20\text{ dB}$ . Results are pictured on figure 4. For the pure dipole model, the anisotropy of the estimation error is clearly seen. Also visible is the increasing estimation variance with increasing complexity, and estimated position lying on a circle for the last case, where the FIM is singular.

#### 4.3. Mixture of monopole and dipole

Finally, figure 5 shows the results of the localization of a mixture of monopole and dipole (with  $a = b = c = 1$ ), for a monopole+dipole, and a monopole+dipole+quadrupole model. Also visible here is the estimated position lying on a circle for the dipole+quadrupole model, where the FIM is singular.

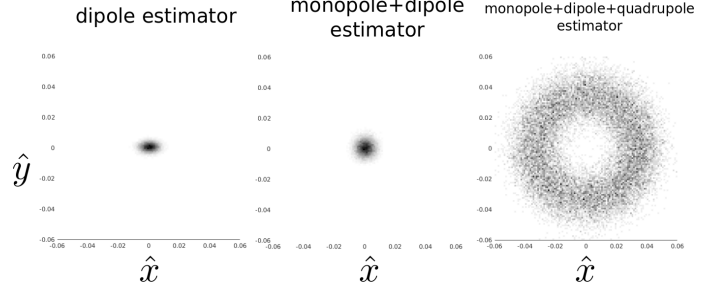


**Fig. 4.** Estimation of the position of a dipole using models of increasing complexity.

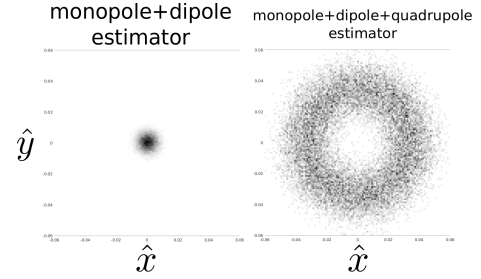


**Fig. 5.** Estimation of the position of a dipole using models of increasing complexity.

#### 4.4. Physical interpretation

The increased variance with increasing complexity of the model is a consequence of the Graf addition theorem. This theorem gives an expansion of a multipole at a given position as a sum of multipoles at a different position. For small distance between this position and the actual position, the terms of degree larger than 1 can be neglected, and a monopole at the center is very similar to an off-centered monopole + dipole with appropriate amplitudes. Including quadrupoles improves the approximation to larger distances, explaining the increasing variance with increasing approximation order. The circular shape of the scatter plot of the estimation is however yet to be explained.

### 5. CONCLUSION

Cramér-Rao bounds for anisotropic sources localization were derived. In particular, it was shown that the variance of the estimation position increases with the complexity of the model, and that, in general, the Fisher information matrix is singular when the model is more complex than the source to be localized. A good match between the source and the model is therefore crucial to ensure good localization performances, as a mismatch does not only imply a larger variance of the estimated positions, but also the impossibility of an unbiased estimation with finite variance.

## 6. REFERENCES

- [1] M. S. Howe, *Theory of Vortex Sound*, Cambridge University Press, Cambridge, 2002.
- [2] B. B. Monson, E. J. Hunter, and B. H. Story, “Horizontal directivity of low- and high-frequency energy in speech and singing,” *The Journal of the Acoustical Society of America*, vol. 132, no. 1, pp. 433–441, 2012.
- [3] F. Shahbazi Avarvand, A. Ziehe, and G. Nolte, “MUSIC algorithm to localize sources with unknown directivity in acoustic imaging,” in *2011 IEEE International Conference on Acoustics, Speech and Signal Processing (ICASSP)*, May 2011, pp. 2744–2747.
- [4] G. Chardon, “A block-sparse MUSIC algorithm for the localization and the identification of directive sources,” in *Proceedings of International Conference on Acoustics, Speech and Signal Processing (ICASSP) 2014*, 2014.
- [5] F. Ollivier, A. Peillot, G. Chardon, and L. Daudet, “Acoustic sources joint localization and characterization using compressed sensing,” *The Journal of the Acoustical Society of America*, vol. 131, no. 4, pp. 3257–3257, 2012.
- [6] B. M. Radich and K. M. Buckley, “EEG dipole localization bounds and MAP algorithms for head models with parameter uncertainties,” *IEEE Transactions on Biomedical Engineering*, vol. 42, no. 3, pp. 233–241, March 1995.
- [7] G. Chardon, Th. Nowakowski, J. de Rosny, and L. Daudet, “A blind dereverberation method for narrowband source localization,” *Journal of Selected Topics in Signal Processing*, vol. 9, pp. 815–824, 2015.
- [8] S. Kitić, L. Albera, N. Bertin, and R. Gribonval, “Physics-driven inverse problems made tractable with cosparsity regularization,” *IEEE Transactions on Signal Processing*, vol. 64, no. 2, pp. 335–348, Jan. 2016.
- [9] I. Dokmanić and M. Vetterli, “Room helps: Acoustic localization with finite elements,” in *2012 IEEE International Conference on Acoustics, Speech and Signal Processing (ICASSP)*, March 2012, pp. 2617–2620.
- [10] J. Le Roux, P.T. Boufounos, K. Kang, and J.R. Hershey, “Source localization in reverberant environments using sparse optimization,” in *IEEE International Conference on Acoustics, Speech and Signal Processing (ICASSP)*, May 2013, pp. 4310–4314.
- [11] E. G. Williams, Ed., *Fourier acoustics*, Academic Press, London, 1999.
- [12] M. Abramowitz and I. Stegun, *Handbook of Mathematical Functions*, Dover Publications, 1965.
- [13] N. A. Gumerov and R. Duraiswami, “Recursions for the computation of multipole translation and rotation coefficients for the 3-D Helmholtz equation,” *SIAM Journal on Scientific Computing*, vol. 25, no. 4, pp. 1344–1381, 2004.
- [14] P. Stoica and T. L. Marzetta, “Parameter estimation problems with singular information matrices,” *IEEE Transactions on Signal Processing*, vol. 49, no. 1, pp. 87–90, Jan 2001.